大韓土木學會論文集
第12卷 第4-1號 · 1992年 12月
pp. 137~151

非線形 造波理論

Nonlinear Theory for Laboratory Wave Generation

金 泰 麟*
Kim, Tae In*

要 旨

可變吃水를 갖는 힌지型 造波機에 의한 造波現象을 다룬 2次解가 提示되었다. 피스톤型 造波機의 경우도 無限吃水를 갖는 힌지型 造波機의 경우로서 함께 취급되었다. 2차해는 平面造波板에 의해 生成되는 波가 서로다른 波速을 갖는 스토우크스 2次波와 2次自由進行波로 構成됨을 보여준다. 2次 自由進行波의 振幅은 淺海領域에서 상대적으로 크고, 深海領域에서는 스토우크波 振幅의 10% 이내로 減小한다. 깊은 吃水를 갖는 (水路바닥 가까이 힌지点이 있는) 造波機일수록 淺海와 中間水深 領域에서 振幅이 작은 自由進行波를 生成하나, 深海域에서는 그와 반대의 現象을 보인다.

Abstract

A complete solution, exact to second-order, for wave motion forced by a hinged-wavemaker of variable-draft is presented. A solution for a piston type wavemaker is also obtained as a special case of a hinged-wavemaker. The laboratory waves generated by a plane wave board are shown to be composed of two components; viz., a Stokes second-order wave and a second-harnomic free wave which travels at a different speed. The amplitude of the second-harmonic free wave is relatively large in shallow water and decreases to less than 10% of the amplitude of the primary wave in deep water. Wavemakers with relatively deeper draft (i.e., hinged near the bottom) generate the free waves of smaller amplitude in shallow and intermediate water depths than the wavemakers with shallow draft. However, the opposite is predicted by theory in deep water.

1. INTRODUCTION

Following the classical wavemaker theory of Havelock[1], Biesel and Suquet[2] solved the linearized wave motions for both a piston-type wavemaker and a flap-type wavemaker hinged on the channel bottom. Later Hyun[3] extended the work of Biesel and Suquet[2] to the case of hinged-wavemakers with a flap of variable-draft. The solution presented by Hyun[3] was extended by Hudspeth and Chen[4] to a wave flume which consisted of two constant depths connected by a gradually sloping transition region. When relatively long waves of finite amplitudes are generated by a sinusoidally moving wavemaker, it has been observed [Goda and Kikuya[5]; Multer and Galvin[6]; Iwagaki

* 정회원 · 陸軍士官學校 土木工學科

and Sakai[7]] that the resultant wave, rather than being of permanent form, breaks down into a primary wave and one or more secondary waves. This secondary wave phenomenon is not predicted in linear wavemaker theories and has stimulated the need for developing nonlinear theories.

Fontanet[8] first developed a complete second-order theory in Lagrangian coordinates for the waves generated by a sinusoidally moving plane wavemaker. However, his solution is relatively complicated to use and results are presented only for piston-type wavemakers. Madsen[9] obtained a more useful approximate solution using a Stokes expansion for a piston-type wavemaker. However, his second-order solution completely neglects the effects of the first-order evanescent eigenmodes, so that the results are valid only for long waves. Multer[10] solved the piston-type wavemaker problem numerically. Daugaard[11] and Massel[12] included the effects of the first-order evanescent eigenmodes in a Stokes expansion formalism to obtain a second-order solution for a piston-type wavemaker. However, their second-order solution still neglects the effects of the first-order evanescent eigenmodes on the free-surface boundary conditions near the wavemaker. Flick and Guza[13] investigated the motion of a flap-type wavemaker by computing the coefficients for the propagating eigenmode numerically. Closed-form expressions for the coefficients in their second-order solution were not presented.

More recently, Kim and Hudspeth[14] presented a complete second-order analytical solution which satisfies exactly the second-order boundary conditions. They used the solution to compute the linear and second-order hydrodynamic pressure force and moment on hinged wavemakers of variable-draft.

In this paper, the first- and second-order analytical solutions for the fluid motion forced by a sinusoidally moving planar wavemaker follow Kim and Hudspeth.[14] Surface wave profiles and the amplitude of the second-harmonic free wave are examined in detail. The analytical results are compared with the limited experimental data.

2. NONLINEAR WAVEMAKER THEORY

2.1 Basic Equations (Kim and Hudspeth, 1990)

For convenience, all physical variables(denoted by *) will be made dimensionless by the following;

$$(x,y,h,d,e,L)=k^*(x^*,y^*,h^*,d^*,e^*,L^*)$$
$$(t,T)=\sqrt{g^*k^*}\,(t^*,T^*),\quad (H,\eta,S,\xi)=(H^*,\eta^*,S^*,\xi^*)/a^*$$
$$(u,v)=(u^*,v^*)/(a^*\sqrt{g^*k^*}),\quad \Phi=\Phi^*/(a^*\sqrt{g^*/k^*})$$
$$B=B^*/(a^*g^*),\quad p=p^*/(\rho^*a^*g^*)$$

in which a^*=amplitude of the first-harmonic wave component and $k^*(=2\pi/L^*)$=the wave number, and g^*=gravitational acceleration.

Consider two-dimensional, irrotational motion of an inviscid, incompressible fluid in a semi-infinite channel($0\le x\le\infty$) of constant water depth, h. The Cartesian coordinate system and the wavemaker configuration are shown in Figure 1. The fluid motion may be obtained from a velocity potential $\Phi(x,y,t)$ according to

$$u(x,y,t)=-\Phi_x,\quad v(x,y,t)=-\Phi_y \qquad (1a,1b)$$

in which the subscripts denote partial differentiation.

The velocity potential, $\Phi(x,y,t)$, is governed by the Laplace equation

$$\Phi_{xx}+\Phi_{yy}=0\ ;\ 0\le x<\infty,\ -h\le y\le\varepsilon\eta(x,t) \qquad (2a)$$

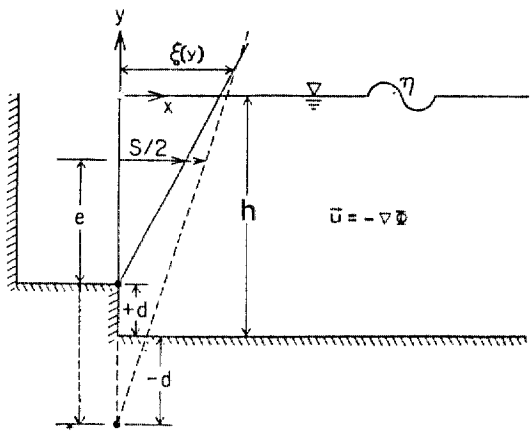

Fig. 1. Definition sketch : Typical wave flume with variable-draft hinged wavemaker

with the boundary conditions

$$\Phi_y=0\ ;\ 0\le x<\infty,\ y=-h \tag{2b}$$

$$\Phi_{tt}+\Phi_y-(\varepsilon\frac{\partial}{\partial t}-\frac{1}{2}\varepsilon^2\nabla\Phi\cdot\nabla)\mid\nabla\Phi\mid^2 +B_t=0\ ;\ 0\le x<\infty,\ y=\varepsilon\eta(x,t) \tag{2c}$$

$$\Phi_x-\varepsilon\Phi_y\chi_y+\chi_t=0\ ;\ x=\varepsilon\chi(y,\ t) \tag{2d}$$

$$\text{Radiation condition}\ ;\ x\to\infty \tag{2e}$$

in which B(t)=Bernoulli constant, the gradient operator $\nabla(\cdot)=(i\frac{\partial}{\partial x}+j\frac{\partial}{\partial y})(\cdot)$ and the small parameter $\varepsilon=ak\ll1$. The wavemaker boundary condition, Eq.(2d), states that the water particles on the wave board must remain on the moving boundary at all times. The instantaneous wave board displacement from its mean position, $\chi(y,t)$, is given by

$$\chi(y,t)=\xi(y)\sin\omega t \tag{3}$$

in which $\omega=2\pi/T$ being the angular frequency of wavemaker oscillation.

The prescribed amplitude of wavemaker displacement, $\xi(y)$, is

$$\xi(y)=\begin{cases}-(S/2)\{(y+h-d)/e\}\cdot U(y+h-d) & \text{for a hinged flap} \quad (4a)\\ -S/2 & \text{for a piston} \quad (4b)\end{cases}$$

in which S/2=wavemaker stroke measured at arbitrary height, e, above hinge, and U(·)=Heaviside step function. In Eq.(2e), the radiation condition requires that only waves traveling in the positive x direction exist far from the wavemaker.

The free-surface profile, $\eta(x,t)$, is given by the free-surface dynamic condition as

$$\eta(x,t)=\Phi_t-\frac{1}{2}\varepsilon\mid\nabla\Phi\mid^2+B\ ;\ 0\le x<\infty,\ y=\varepsilon\eta(x,t) \tag{5}$$

The pressure, p, is determined from the Bernoulli equation given by

$$p(x,y,t)=\Phi_t-\frac{1}{2}\varepsilon\mid\nabla\Phi\mid^2-y/\varepsilon+B\ ;\quad 0\le x<\infty,\ -h\le y\le\varepsilon\eta \tag{6}$$

The free-surface conditions, Eqs.(2c) and (5), and the wavemaker boundary condition, Eq.(2d), may be expressed by their values at mean positions by use of Taylor's theorem: i.e.,

$$\sum_{n=0}^{\infty}\frac{(\varepsilon\eta)^n}{n!}\frac{\partial^n}{\partial y^n}[\Phi_{tt}+\Phi_y-(\varepsilon\frac{\partial}{\partial t}-\frac{1}{2}\varepsilon^2\nabla\Phi\cdot\nabla)\mid\nabla\Phi\mid^2]=0;\ y=0 \tag{7}$$

$$\eta-\sum_{n=0}^{\infty}\frac{(\varepsilon\eta)^n}{n!}\frac{\partial^n}{\partial y^n}[\Phi_t-\frac{1}{2}\varepsilon\mid\nabla\Phi\mid^2+B]=0;\ y=0 \tag{8}$$

and

$$\sum_{n=0}^{\infty}\frac{(\varepsilon\eta)^n}{n!}\frac{\partial^n}{\partial x^n}[\Phi_x-\varepsilon\Phi_y\chi_y+\chi_t]=0;\ x=0 \tag{9}$$

In addition, the unknowns Φ, η, B, and p may be expanded in the small parameter, ε, in the following:

$$\Phi(x,y,t)=\sum_{n=0}^{\infty}\varepsilon^n{}_{n+1}\Phi(x,y,t) \tag{10a}$$

$$\eta(x,t)=\sum_{n=0}^{\infty}\varepsilon^n{}_{n+1}\eta(x,t) \tag{10b}$$

$$B(t)=\sum_{n=0}^{\infty}\varepsilon^n{}_{n+1}B(t) \tag{10c}$$

$$p(x,y,t)=p_s(y)+\sum_{n=0}^{\infty}\varepsilon^n{}_{n+1}p(x,y,t) \tag{10d}$$

in which $p_s=-y/\varepsilon$ represents the dimensionless hydrostatic pressure.

In laboratory waves, the wave frequency is fixed and therefore the wave number will change as the wave amplitude increases. Since the spatial variables, x* and y*, are made dimensionless by the wave number, k*, the wave frequency, ω*, must be perturbed in order to obtain the correction terms, and then the equality of wave frequency may be introduced in order to obtain the change in the wave number [cf. Goda and Abe (15), p. 18]. A dimensionless time variable is defined by

$$\tau=\omega t=(\sum_{n=0}^{\infty}\varepsilon^n\ \omega_n)t \tag{11}$$

Upon substitution of Eqs.(7)-(11) into Eqs.(2)-(6) and collection of the terms of the same order in ε, a set of linear boundary value problems is obtained which may be solved in successive order.

2.2 Linear Solution

The linear boundary value problem obtained for order ε^0 from the perturbation expansion is as

follows:

$$_1\Phi_{xx}+{}_1\Phi_{yy}=0 \quad ; 0\le x<\infty,\ -h\le y\le 0 \tag{12a}$$
$$_1\Phi_y= \quad ; 0\le x<\infty,\ y=-h \tag{12b}$$
$$\omega_o^2\ {}_1\Phi_{\tau\tau}+{}_1\Phi_y+\omega_o\ {}_1B_\tau=0:\ 0\le x<\infty,\ y=0 \tag{12c}$$
$$_1\Phi_x=-\omega_o\chi_\tau \quad ; x=0,\ -h\le y\le 0 \tag{12d}$$
$$\text{Radiation condition } x\to\infty \tag{12e}$$

in which $\chi(y,\tau)=\xi(y)\sin\tau$.

The first-order free-surface elevation, $_1\eta$, and the dynamic pressure are obtained according to

$$_1\eta=\omega_o\ {}_1\Phi_\tau \quad ; 0\le x<\infty,\ y=0 \tag{13}$$

and

$$_1p=\omega_o\ {}_1\Phi_\tau \quad ; 0\le x<\infty,\ -h\le y\le 0 \tag{14}$$

A simple-harmonic solution to the linear problem requires that $_1B$ be identically zero in Eq.(12 c). The linear solution is well-known and is given by the following eigenfunction expansion [cf. Wehausen(16) and Hudspeth and Chen[4]].

$$_1\Phi(x,y,\tau)=a_1\phi_1(y)\sin(x-\tau)$$
$$+\cos\tau\sum_{m=2}^{\infty}\alpha_\mu\phi_m(y)\ \exp(-\alpha_m\ x) \tag{15}$$

in which the orthonormal eigenfunctions, $\phi_1(y)$ and $\phi_m(y)$, in the interval of orthogonality, $-h\le y\le 0$, are given by

$$\phi_1(y)=\cosh(y+h)/n_1$$
$$;\ \phi_m(y)=\cos\alpha_m(y+h)/n_m \ \text{ for } m>2 \tag{16}$$

and the normalizing constants are

$$n_1^2=\int_{-h}^{0}\cosh^2(y+h)dy=[2h+\sinh(2h)]/4 \tag{17a}$$

and

$$n_m^2=\int_{h}^{0}\cos^2\alpha_\mu(y+h)dy=$$
$$[2\alpha_m h+\sin(2\alpha_m h)\}/(4\alpha_m) \ \text{ for } m>2 \tag{17b}$$

The wave number, k, and the dimensionless eigenvalues, m, in Eq.(15) are determined from Eq. (12c) and are given by the real root(roots) of the transcendental equation

$$\omega_o^2=\tanh\ h \tag{18a}$$

and

$$\omega_o^2=-\alpha_m\ \tan\ \alpha_m h \qquad \text{for } m>2 \tag{18b}$$

respectively.

Far away from the wavemaker (x>3h, say), the evanescent eigenmodes in Eq.(15) are sensibly less than 1% of their values at the wavemaker (x=0), and the dimensionless linear free-surface profile, $_1\eta(x,t)$, is given by

$$_1\eta=\cos(x-\tau) \tag{19}$$

so that the dimensionless wavemaker gain function, $S(=S^*/a^*)$, is determined from Eq.(13) to be

$$S=2\ en_1^2/D(h) \tag{20}$$

in which $D(h)=\sinh h\cdot[(h-d)\sinh h-\cosh h+\cosh\{d\cdot U(d)\}]$.

For a piston-type wavemaker, $(-d \text{ and } e)\to\infty$, and Eq.(20) reduces to

$$S=2n_1^2/\sinh^2 h \tag{21}$$

in agreement with Eq.(13) given by Madsen(9).

The coefficients a_1 and a_m in Eq.(15) are determined from the wavemaker boundary condition, Eq.(12d), and are given by

$$a_1=-\omega_o n_1/\sinh\ h$$
$$\text{for both a hinged flap and a piston} \tag{22a}$$

and

$$a_m=\begin{cases}\omega_o\ n_1^2\ D_m(\alpha_m)/[\alpha_m^3 n_m D(h)] \\ \text{for a hinged flap} \\ \omega_o\ n_1^2\ \sin\ \alpha_m/[\alpha_m^2 n_m\ \sinh^2 h] \\ \text{for a piston}\end{cases} \tag{22b}$$

in which $D_m(\alpha_m)=\alpha_m(h-d)\sin\alpha_m h+\cos\alpha_m h-\cos\{\alpha_m d\cdot U(d)\}$.

2.3 Second-Order Solution

The boundary value problem at second-order is the following fororder ε:

$$_2\Phi_{xx}+{}_2\Phi_{yy}=0 \quad ; 0\le x<\infty,\ -h\le y\le 0 \tag{23a}$$
$$_2\Phi_y=0 \quad ; 0\le x<\infty,\ y=-h \tag{23b}$$
$$\omega_o^2\Phi_{\tau\tau}+{}_2\Phi_y+\omega_o\ {}_2B_\tau=-2\omega_o\omega_1\ {}_1\Phi_{\tau\tau}+\omega_o\frac{\partial}{\partial\tau}$$
$$(_1\Phi^2{}_x+{}_1\Phi_y{}^2)-{}_1\eta\frac{\partial}{\partial y}(\omega_o^2\ {}_1\Phi_{\tau\tau}+{}_1\Phi_y)$$

$$; \ 0 \le x < \infty, \ y = 0 \qquad (23c)$$

$${}_2\Phi_x = -\omega_1 \chi_\tau + {}_1\Phi_y \chi_y - {}_1\Phi_{xx} \chi; \ x = 0, \ -h \le y \le 0 \qquad (23d)$$

Radiation condition $x \to \infty$ (23e)

The dimensionless free-surface elevation, ${}_2\eta$, and the dimensionless dynamic pressure, ${}_2p$, are given by

$${}_2\eta = \omega_{02}\Phi_\tau + \omega_1 {}_1\Phi_\tau - \frac{1}{2}({}_1\Phi_x{}^2 + {}_1\Phi_y{}^2) + \omega_0 {}_1\eta_1 \Phi_{y\tau} + {}_2B \ ; \ 0 \le x < \infty, \ y = 0 \qquad (24)$$

and

$${}_2p = \omega_{02}\Phi_\tau + \omega_1 {}_1\Phi_\tau - \frac{1}{2}({}_1\Phi_x{}^2 + {}_1\Phi_y{}^2) + {}_2B \ ; \ 0 \le x < \infty, \ -h \le y \le 0 \qquad (25)$$

Previously published solutions [Madsen[9]; Daugaard[11]; Flick and Guza[13]; and Massel[12]] have failed to include the time-independent trms in Eqs.(23c) and (23d) as well as the near-field evanescent terms in Eq.(23c).

Taking the time average of both sides of Eq.(24) over one wave cycle and requiring that $\langle {}_2\eta \rangle = 0$ {$\langle \cdot \rangle$ represents a temporal average equal to $\frac{1}{T}\int_0^T (\cdot)dt$} in the region $x > 3h$, the Bernoulli constant at second-order is determined to be

$${}_2B = \frac{ak}{2 \sinh 2h} \qquad (26)$$

Accordingly, ${}_2B_\tau = 0$ in Eq.(23c). In addition, the first term in the right hand side of Eq.(23c) must vanish since the term $\omega_0\omega_{11}\Phi_{\tau\tau}$ would introduce a non-periodic term of the form, $\tau_1\Phi$, in the solution for ${}_2\Phi$. Since $\omega_0 \neq 0$, it is required that

$$\omega_1 = 0 \qquad (27)$$

showing that the wave number, k, is a constant correct to second-order.

For Eqs.(23), the second-order solution may be decomposed into four linear velocity potentials ; namely, a Stokes wave potential, ${}_2\Phi^s$; a near-field evanescent interaction potential, ${}_2\Phi^e$; a wavemaker-free wave potential, ${}_2\Phi^f$; and a time-independent potential, Ψ; i.e.,

$${}_2\Phi = {}_2\Phi^s + {}_2\Phi^e + {}_2\Phi^f + \Psi \qquad (28)$$

Substitution of Eqs.(15) and (28) into Eqs.(23c and d) gives

$$L\{{}_2\Phi^s + {}_2\Phi^e + {}_2\Phi^f + \Psi\} = f_1(\phi_1)\sin 2(x-\tau) + f_2(\phi_1, \phi_m)\exp(-\alpha_m x)\sin(x-2\tau) + f_3(\phi_1, \phi_m)\exp(-\alpha_m x)\cos(x-\tau) + f^4(\phi_m, \phi_n)\exp\{-(\alpha_m+\alpha_n)x\}\sin 2\tau + f_5(\phi, \phi_m)\exp(-\alpha_m x)\cos x \ ; \ 0 \le x < \infty, \ y = 0 \qquad (29a)$$

and

$$\frac{\partial}{\partial x}\{{}_2\Phi^s + {}_2\Phi^e + {}_2\Phi^f + \Psi\} = W_1(\phi_1, \xi)\cos 2\tau + W_2(\phi_m, \xi)\sin 2\tau + W_3(\phi_1, \xi) \ ; \ x = 0, \ -h \le y \le 0 \qquad (29b)$$

in which the linear operator $L(\cdot) = \{\omega_0{}^2\frac{\partial^2}{\partial\tau^2} + \frac{\partial}{\partial y}\}(\cdot)$, and the terms f_1, f_2, f_3, f_4, f_5, w_1, w_2, and w_3 represent the first-order non-linear interactions. It should be pointed out that the first-order evanescent eigenmodes form part of forcing functions at the second-order in Eqs.(29). This point has been neglected in earlier nonlinear wavemaker theories.

Now if the Stokes wave potential, ${}_2\Phi^s$, satisfies exactly Eqs.(23a, b, and e) as well as the free-surface condition, $L({}_2\Phi^s) - f_1(\phi_1) \sin 2(x-\tau) = 0$, the near-field evanescent wave potential, ${}_2\Phi^e$, may be chosen to satisfy Eqs.(23a, b, and e) in addition to the free-surface condition, $L({}_2\Phi^e) - f_2(\phi_1, \phi_m)\exp(-\alpha_m x)\sin(x-\tau) - f_3(\phi_1, \phi_m)\exp(-\alpha_m x)\cos(x-2\tau) - f_4(\phi_m, \phi_n)\cdot\exp(-\alpha_m x)\sin(x-2\tau) = 0$. The time-independent potential, Ψ, must satisfy Eqs.(23a, b, and e) as well as the two inhomogeneous boundary conditions ; $L(\Psi) - f_5(\phi_1, \phi_m)\exp(-\alpha_m x)\cos x = 0$ on $y = 0$, and $\frac{\partial}{\partial x}(\Psi - W_3(\Phi_1, \xi) = 0$ at $x = 0$. Then the free wave potential, ${}_2\Phi^f$, must satisfy Eqs.(23a, b, and e) as well as

$$L\{{}_2\Phi^f\} = 0 \ ; \ 0 \le x < \infty, \ y = 0 \qquad (30a)$$

and

$${}_2\Phi_x{}^f = -({}_2\Phi_x{}^s x + {}_2\Phi_x{}^e) + W_1(\phi_1, \xi)\cos 2\tau + W_2(\phi_m, \xi)\sin 2\tau \ ; \ x = 0, \ -h \le y \le 0 \qquad (30b)$$

which gives a well-posed Sturm-Liouville problem for the second-order free wave potential, ${}_2\Phi^f$, in

the vertical y coordinate.

The Stokes wave potential, ${}_2\Phi^s$, is simply the Stokes second-order solution given by Stokes[17]

$$\varepsilon_2\Phi^s = -\frac{3ak\omega_o}{8}\frac{\cosh 2(y+h)}{\sinh^4 h}\sin 2(x-\tau) \qquad (31)$$

The solution for the near-field evanescent1 wave potential, ${}_2\Phi^e$, and the free secondary wave potential, ${}_2\Phi^f$, are assumed to be given by

$$\varepsilon_2\Phi^e(x,y,t) =$$

$$\sum_{m=2}^{\infty}\{E_m[\phi_1(y)\phi_m(y)\cos(x-2\tau)-\phi_1'(y)\phi_m'(y)\sin(x-2\tau)]+F_m[\phi_1(y)\phi_m(y)\sin(x-2\tau)+\phi_1'(y)\phi_m'(y)\cos(x-2\tau)]\}\exp[-\alpha_m x]+\sum_{m=2}^{\infty}\sum_{n=2}^{\infty}G_{mn}[\phi_m(y)\phi_n(y)-\phi_m'(y)\phi_n'(y)]\exp[-(\alpha_m+\alpha_n)x]\cdot\sin 2\tau \qquad (32)$$

and

$$\varepsilon_2\Phi^f(x,y,t)=[B_1\cos(\beta_1 x-2\tau)+C_1\sin(\beta_1 x-2\tau)]Q_1(y)+\sum_{n=2}^{\infty}[B_n\sin 2\tau+C_n\cos 2\tau]\,Q_n(y)\exp[-\beta_n x] \qquad (33)$$

in which the orthonormal eigenfunctions, $Q_1(y)$ and $Q_n(y)$, in the interval of orthogonality, $-h\le y\le 0$, are

$$Q_1(y)=\cosh\beta_1(y+h)/N_1;\quad Q_n(y)=\cos\beta_n(y+h)/N_n \qquad (34)$$

and the normalizing constants are

$$N_1^2=\int_{-h}^{0}\cosh^2\beta_1(y+h)dy=[\beta_1 h+\sinh(2\beta_1 h)][4\beta_1] \qquad (35a)$$

$$N_n^2=\int_{-h}^{0}\cos^2\beta_n(y+h)dy=[2\beta_n h+\sin(2\beta_n h)][4\beta_n] \qquad (35b)$$

The eigenvalues, β_1 and β_n, are the real roots of

$$4\omega_0^2=\beta_1\tanh\beta_1 h \qquad (36a)$$

and

$$4\omega_0^2=-\beta_n\tan\beta_n h \quad \text{for} \quad n\ge 2 \qquad (36b)$$

respectively. In Eq.(32), $\phi_1'(y)=\sinh(y+h)/n_1$ and $\phi_m'(y)=\sin\alpha_m(y+h)/n_m$.

The coefficients E_m, F_m, and G_{mn} in Eq.(32) are determined from the free-surface boundary condition for ${}_2\Phi^e$. The final closed-form expressions for these coefficients are given by

$$E_m=2ak\omega_0\frac{n_1^3\ D_m(\alpha_m)[B_m(\alpha_m)-A_m(\alpha_m)]}{D(h)\ \sinh h\ \alpha_m^2\ n_m\ [4+A_m^2(\alpha_m)]} \qquad (37a)$$

$$F_m=-ak\omega_0\frac{n_1^3\ D_m(\alpha_m)[4+A_m(\alpha_m)\cdot B_m(\alpha_m)]}{D(h)\ \sinh h\ \alpha m^2\ n_m\ [4+A_m^2(\alpha_m)]} \qquad (37b)$$

$$G_{mn}=ak\omega_0\frac{n_1^4}{2D^2(h)}\cdot\frac{D_m(\alpha_m)D_n(\alpha_n)[2+2\omega_0^4/\alpha_m\alpha_n+\alpha_n/(\alpha_m\cos^2\alpha_m h)]}{\alpha m^2\alpha_n^2 n_m n_n(2-4\omega_0^4/\alpha_m\alpha_n-\alpha_m/\alpha_n-\alpha_n/\alpha_m)} \qquad (37c)$$

in which $A_m(\alpha_m)=4\omega_o^4\alpha_m^{-1}-\alpha_m^{-1}+\alpha_m$ and $B_m(\alpha_m$ and $B_m(\alpha_m)=\frac{1}{2}(\alpha_m^{-1}\ \operatorname{sech}^2 h-4\omega_o^4\alpha_m^{-1}-\alpha_m\ \sec^2\alpha_m h)$.

Likewise the coefficients B_1, B_n, C_1, and C_n in Eq.(33) are determined from the kinematic wavemaker boundary condition for ${}_2\Phi^f$ given by Eq.(29 b). The final closed-form expressions for these coefficients are given in Appendix I. It should be noted that the first-order evanescent eigenmodes significantly affect the values of B_1 and C_1 in Eqs. (51a, c). Since B_1 and C_1 represent the amplitude of the propagating second-harmonic free wave in Eq.(33), first-order evanescent eigenmodes play the important role in generating second-harmonic free wave, though they vanish far away from the wavemaker. The coefficients for a poston-type wavemaker may be obtained by taking the limit in Eqs.(50a)~(50p) for the valus of $d=-\infty$.

A feature of the second-order problem is the time-independent potential, $\Psi(x,y)$, in Eq.(28). The time-independent potential, Ψ, must satisfy the following boundary value problem:

$$\Psi_{xx}+\Psi_{yy}=0 \quad ;\ 0\le x<\infty,\ -h\le y\le 0 \qquad (38a)$$

$$\Psi_y=-\frac{1}{2}a_1\omega_o\phi_1(0)\sum_{m=2}^{\infty}a_m\phi_m(0)(\operatorname{sech}^2 h+\alpha_m^2\sec^2\alpha m_h)\exp(-\alpha_m x)\cos x \quad ;\ 0\le x<\infty,\ y=0 \qquad (38b)$$

$$\Psi_y=0 \quad ;\ 0\le x<\infty,\ y=-h \qquad (38c)$$

$$\left[-\frac{Sa_1}{4e}[\phi_1'(y)+(y+h-d)\phi_1(y)]\cdot U(y+h\right.$$

$$\Psi_x = \begin{cases} -\ d) \text{ for a hinged flap} \\ \qquad ;\ x=0,\ -h\le y<0 \qquad (38d) \\ -\dfrac{S}{4}\, a_1\phi_1(y) \text{ for a piston} \end{cases}$$

$$\Psi_x \to \text{bounded} ;\ x \to +\infty \qquad (38e)$$

Again, Ψ may be decomposed into two independent potentials; namely,

$$\Psi = \Psi^{fs} + \Psi^{wm} \qquad (39)$$

The free-surface potential, Ψ^{fs}, is chosen to satisfy Eqs.(38a, b, c, and e) regardless of the condition of the wavemaker. Then the wavemaker potential, Ψ^{wm}, must satisfy Eqs.(38a, c, and e) as well as the homogeneous free-surface boundary condition

$$\Psi^{wm}_{\bar{y}} = 0 \qquad ;\ 0\le x<\infty,\ y=0 \qquad (40a)$$

and the inhomogeneous wavemaker boundary condition

$$\Psi^{wm}_x = -\Psi^{fs}_x + w_3(\phi_1,\ \xi) ;\ x=0,\ -h\le y\le 0 \qquad (40b)$$

in which $w_3(\phi_1, \xi)$ is given by the right hand side of Eq.(38d).

The solutions for Ψ^{fs} and Ψ^{wm} may be given by

$$\varepsilon\Psi^{fs}(x,y) = \sum_{m=2}^{\infty} \{b_m[\phi_1(y)\cos x - \phi_1'(y)\phi_m'(y)\sin x] + c_m[\phi_1(y)\phi_m(y)\sin x + \phi_1'(y)\phi_m'(y)\cos x]\}\exp(-\alpha_m x) \qquad (41)$$

and

$$\varepsilon\Psi^{wm}(x,y) = A_o x + \sum_{n=1}^{\infty} A_n\varphi_n(y)\exp(-\mu_n x) \qquad (42)$$

in which the orthonormal eigenfunctions, $\varphi_n(y)$, in the interval of orthogonality, $-h\le y\le 0$, are $\varphi_n = \sqrt{h/2}\cdot\cos\mu_n(y+h)$ provided that the eigenvalues are $\mu_n = n\pi/h$.

Substituting Eq.(41) into Eq.(38b) and equating the coefficients of cos x and sin x on both sides, b_m and c_m are determined to be

$$b_m = ak\omega_o \frac{D_m(\alpha_m)H_m(\alpha_m)}{D(h)\phi_1^2(0)\phi_1'(0)\alpha_m n_m^3\phi_m^2(0)} \qquad (43a)$$

and

$$c_m = -\frac{1}{2}\, ak\omega_o \frac{D_m(\alpha_m)H_m(\alpha_m)(\alpha_m^{-1}-\alpha_m)}{D(h)\phi_1^2(0)\phi_1'(0)\alpha_m n_m^3\phi_m^2(0)} \qquad (43b)$$

in which $H_m(\alpha_m) = (\alpha^{-1}\cos^2\alpha_m h + \cosh^2 h)(\alpha_m + \alpha_m^{-1})^{-2}$.

The coefficients Ao and An are determined from Eq.(40b) and are given by

$$A_o = \frac{1}{2} ak\omega_o\left[\frac{n_1^2(h-d)}{D(h)} - \frac{D_m(\alpha_m)H_m(\alpha_m)(\alpha_m+\alpha_m^{-1})}{D(h)\phi_1^2(0)\alpha_m n_m^3\phi_m(0)}\right] \qquad (44a)$$

and

$$A_n = -ak\omega_o\left\{\frac{(-1)^n n_1^2\phi_1(0)[2+\omega_o^2(h-d)(1+\mu_n^{-2})] + I_5(d)}{\sqrt{2h\ \phi_1^2(0)\cdot D(h)\mu_n^3(1+\mu_n^{-1})^{-2}}} - \frac{(-1)^n}{\sqrt{2h\ \phi_1^2(0)D(h)\mu_n}} \sum_{m=2}^{\infty} \frac{D_m(\alpha_m)H_m(\alpha_m)(1+\alpha_m^{-2})_2(1+\alpha_m^{-2}-\mu_v[\alpha_m^{-2})}{n_m^3\phi_m(0)[(1+\alpha_m^{-2}+\mu_n^2\alpha_m^{-2})^2 - 4\mu_n^2\alpha_m^{-2}}\right\} \qquad (44b)$$

in which

$$I_5(d) = \begin{cases} -n_1^3\ \sqrt{2/h}\ \varphi_n(d-h)\phi_1(d-h)[2+\mu_n(1 \\ \quad -\mu_n^{-2})\tanh d\cdot\tan\mu_n d] \text{ for } d\ge 0 \\ -2n_1^2 \qquad \text{for } d<0. \end{cases} \qquad (44c)$$

This time-independent solution, which has been neglected in former studies, is required to satisfy exactly the inhomogeneous boundary conditions both at the free-surface and at the wavemaker. It is proved that this time-independent solution accurately estimate the mean return flow in a closed wave flume computed by the Eulerian method. This is a feature of the present theory, and the significance of the time-independent solution related to water mass circulation in a closed wave flume has been discussed in detail by Kim et. al.[18].

3. SURFACE WAVE PROFILES

The dimensionless free-surface elevation, $\eta(x,t)$, up to second-order is given by

$$\eta(x,t) = {}_1\eta(x,\ \tau) + \varepsilon_2\eta(x,\tau) \qquad (45)$$

Substituting Eqs.(15), (26), and (28) for ${}_1\Phi$, B, and ${}_2\Phi$ into Eq.(45) and considering the propagating modes only, the dimensionless free-surface

elevation at $x \geq 3h$, is given by

$$\eta(x, \tau)=\cos(x-\tau)+\frac{ak \cosh h}{4\sinh^3 h}(\cosh 2h+2)\cos^2(x-\tau)+2Q_1(0)\{B_1\sin(\beta_1 x-2\tau)-C_1\cos(\beta_1 x-2\tau)\} \quad (46)$$

or

$$\eta(x, \tau)=\cos(x-\tau)+a_2^s \cos 2(x-\tau)+a_2^f \cos(\beta_1 x-2\tau+\delta_1) \quad (47a)$$

in which $\delta_1=\text{ARCTAN}\{(-B_1)/(C_1)\}$ and

$$a_2^s=ak \cosh h(\cosh 2h+2)/(4\sinh^3 h) \quad (47b)$$

$$a_2^f=2Q_1(0)\ (B_1^2+C_1^2)^{1/2} \quad (47c)$$

Thus a free wave of dimensionless amplitude, a_2^f, and dimensionless celerity, $C^f=2/\beta_1$, travels together with the usual Stokes second-order wave in laboratory flumes. Since $\beta_1>2$, the free wave travels at slower speed than the Stokes wave.

The two second-harmonic wave components in Eqs.(47) may be combined to yield

$$\eta(x,\tau)=\cos(x-\tau)+a_2(x) \cos 2[x-\tau+\delta_{11}(x)] \quad (48a)$$

in which

$$a_2^2(x)=(a_2^s)+(a_2^f)^2+2(a_2^s)(a_2^f)\cos[(\beta_1-2)x+\delta_1] \quad (48b)$$

As shown in Eq.(48b), the amplitude of the second-harmonic wave demonstrates a "beat" effect as was first identified experimentally by Hansen and Svendsen[19] as a result of the interactions of the Stokes and the free wave with a dimensionless beat length, L_b, given by $L_b=2\pi/(\beta_1-2)$. The ratios of the free wave celerity to the Stokes wave celerity, C^f/C^s, and the beat length to the first-harmonic wave length, L_b/L, are shown in Figure 2 as functions of the relative water depth, h/L_o.

In shallow water($h/L_o<0.015$), the ratio of C^f/C^s approaches to unity showing that the free wave travels about the same speed as the Stokes wave. Meanwhile, the ratio of L_b/L shows larger than unity in shallow water, showing that the beat length is longer than the Stokes wave length. In deep water, however, the ratios of C^f/C^s and L_b/L approach to 0.5 and 0.05 respectively, showing that

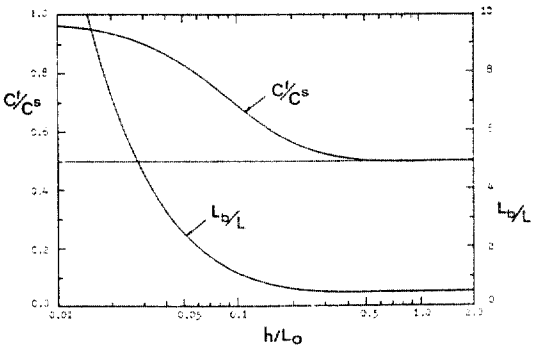

Fig. 2. Dimensionless free wave celerity, C^f/C^s, and beat(meander) length, L_b/L, as functions of the relative water depth

the free wave travels at a half the Stokes wave celerity and that the beat length is only 1/20 of the first-harmonic wave length.

From Eq.(47a), the elevation of the resultant wave crest and trough is given by

$$\eta_{crest}=1+a_2^s+a_f \cos[(\beta_1-2)x+\delta_1] \text{ at } x-\tau=2n\pi;\ n=0,\ 1,\ 2,\ \cdots \quad (49a)$$

$$\eta_{trough}=-1+a_2^s+a_2^f \cos[(\beta_1-2)x+\delta_1] \text{ at } x-\tau=(2n+1)\pi;\ n=0,\ 1,\ 2,\ \cdots \quad (49b)$$

so that the dimensionless wave height, H, is given by

$$H=\eta_{crest}-\eta_{troygh}=2. \quad (50)$$

Therefore, up to second-order, the wave heights measured at fixed locations are independent of the longitudinal distance over the wave flume, and are given by the height of the first-harmonic wave. However, the spatial envelope of the wave train demonstrates a snake-like pattern with the "meander length," L_b.

The waveform in the horizontal distance, x, of the second-order wave componets as well as the resultant wave predicted by Eqs.(48) is shown in Figure 3 for a wave of $H^*=0.692$m, $T^*=3.76$ sec [Case 7-B in Dean[20]], which is forced by a hinged flap on a channel bottom in a wave flume of constant depth, $h^*=4.42$m. The total second-harmonic wave demonstrates a beat effect as shown in Figure(3f). Accordingly, the resultant

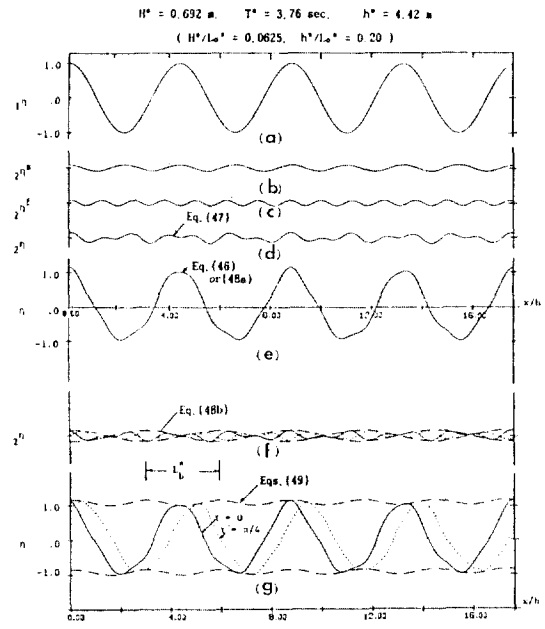

Fig. 3. Propagation of both the second-order wave components and the resultant wave profile along the wave flume

wave becomes irregular in the longitudinal distance, x, as shown in Figure(3e). The solid lines represent the wave profile at $\tau=0$, and the dotted line in Figure(3g) represents the same wave train at $\tau=\pi/4$. As the wave propagates within this spatial envelope, its form continually changes over the "meander length", L_b^*.

Figure 4 shows a sample record of the spatial envelope of wave trains measrued in the Oregon State University Wave Research Laboratory in which wavemaker is a flap hinged at 7.6cm above the channel bottom. The water depth over the main floor was 3.35m. The spatial envelope of wave crest and trough was recorded by moving a wave guage slowly over the main floor of the channel. The meander form in the spatial envelope of the wave crest and trough elevation is evident in Figure 4, with the meander length, $L_b^*=14.2$m which show good agreement with the predicted value 13.2m. The amplitude of the free wave measured from the chart is $a_2'^*=3.4$cm which is in good agreement with theoritical value

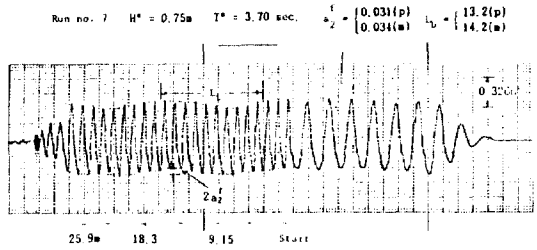

Fig. 4. Sample record of spatial envelope of wave crest and trough elevation in a constant water depth h=3.35m

3.1cm.

Figure 5 shows a comparison between the predicted and the measured surface wave profile at three different locations along the channel for the wave train with a wave height, $H^*=1.07$m and a wave period, $T^*=4.55$ seconds. The existence of the secondary free wave may be readily recognized by the variation of waveforms at different locations. In Figure 5, agreement between the wave guage records and the predicted values by Eq.(47a) is fairly good. The discrepancies between the measured and the predicted values along the down-crossing parts of the wave profile in Figure 5 may be due to the higher-harmonic wave components which are not included in the present second-order theory.

The dimensionless amplitude of the free wave, a_2'/a, is plotted in Figure 6 as a function of the dimensionless wave height, H^*/L_o^*, and the relative water depth, h/L_o (L_o=Deep water wave length) for three types of wavemaker geometry. The effects of the free wave are more pronounced in shallow and intermediate water depths and for waves of larger amplitude. Hinged wavemakers of small drafts (large+d) are shown to produce larger free waves than other types of wavemakers in shallow and intermediate water depths. In deep water, however, the free wave effects are more pronounced for piston-type wavemakers. The amplitude of the free wave shown in Figure 6 is 10% of those of the first harmonic wave in deep water.

Figure 7 shows the ratio of the wave amplitude to the Stokes second- harmonic wave amplitude,

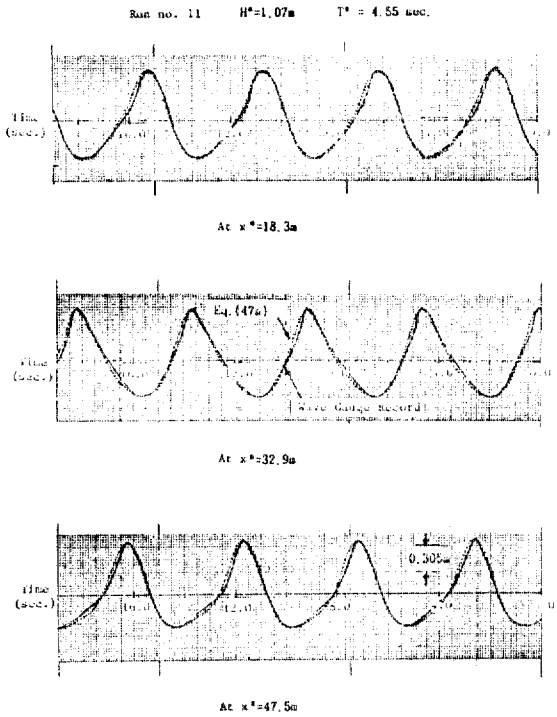

Fig. 5. Comparison between the predicted and the measured surface wave profiles at three different locations

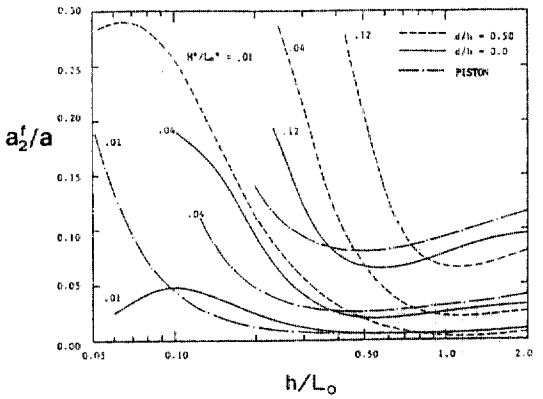

Fig. 6. Dimensionless amplitude of the free wave, a_2^f/a, as a function of the relative water depth

a_2^f/a_2^s, over a range of relative water depths, h/L_o. For flap-type wavemakers hinged on or above the channel bottom ($d/h \geq 0$), the minimum values of af /as occur at shallow water depths between 0.027$<h/L_o<$0.06, while the maximum values occur

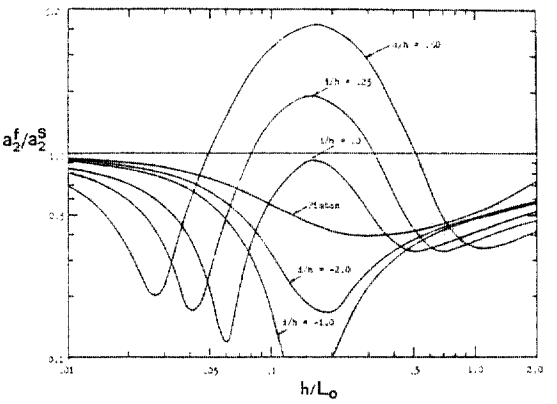

Fig. 7. Ratio of the free wave amplitude to Stokes second-order wave amplitude as a function of the relative water depth

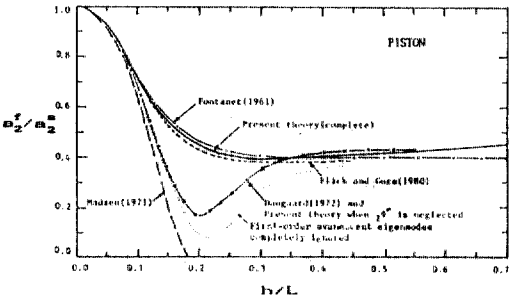

Fig. 8. Comparison of present theory with existing theories for the ratio, a_2^f/a_2^s as a function of the realtive water depth

at $h/L_o=0.16$. For wavemakers hinged below the channel bottom, however, the minimum values of a_2^f/a_2^s occur at intermediate water depths between $0.06<h/L_o<0.3$, while the maximum values occur in the shallow water region. Figure 7 also shows the increasing values of a_2^f/a_s in deep water (h/Lo % 1.0) for piston-type wavemakers.

In Figure 8, the predicted values of a_2^f/a_2^s by Eqs.(48) are compared with the other theoretical values. For piston-type wavemakers, the values of a_2^f/a_2^s given by Eqs. (48) are close to the values predicted by the complete Lagrangian second-order solution of Fontanet[8] in shallow and intermediate water depths. In deep water, however, the present theory gives higher values of af /as than

Fontanet's[8]. The solution of Daugaard[11] is identical with the present theory, when the near-field evanescent potential, ${}_2\Phi^e$, in Eq.(28) is neglected. The shallow water approximate solution of Madsen[9] gives values of a_2^f/a_2^s close to the theories of others only in shallow water region as would be expected. The solution of Flick and Guza[13] also shows close resemblance to that of Fontanet [8], but gives slightly lower values of af/as than both the present theory and Fontanet's. These discrepancies seems to be due to the difference of the number of the first-order evanescent modes included in computation for second-order wave components. [Flick and Guza (13, Fig.4) included 5 10 modes while present theory included 10 30 modes.] Flick and Guza(13, p 87)argued that Dargaard neglected the effects of the first-order evanescent eigenmodes. However, a numerical check by the present theory showed that Daugaard[11] correctly included the first-order evanescent eigenmodes in his second-order solution, although he neglected ${}_2\Phi^e$, as did Madsen[9].

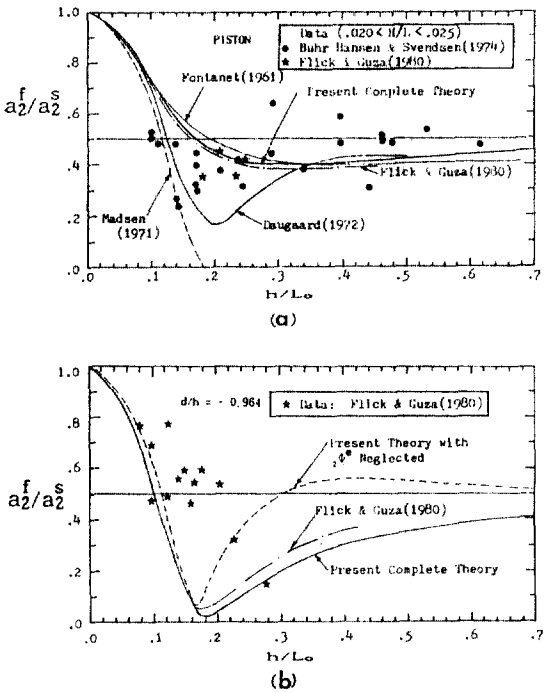

Fig. 9. Comparison of present theory with measured data for the ratio, a_2^f/a_2^s, as a function of the relative water depth

In Figure 9a, measured data for the ratio of the free wave amplitudeto the Stokes second-order wave, a_2^f/a_2^s, reported by Burh Hansen and Svendsen[19] are included. The scatter in the measured data is large, and no theory is confirmed to be superior to others. The errors between most of the data and the present complete theory are within 25% of the predicted values. In Figure 9b, the measured data for the ratio, a_2^f/a_2^s, reported by Flick and Guza[13] for the case of a hinged wavemaker are included. The present theory shows good agreement with the data in shallow water. For the relative water depth $0.12<h/L_o<0.23$, the data show higher values than the predictions of both theories.

4. CONCLUSIONS

A complete solution, exact to second-order, for wave motion forced by a hinged wavemaker of variable draft has been presented. Surface wave profiles in particuler attention to the second-harmonic free wave have been studied. For studying the secondary free wave motion, the influence of forcing by the nonlinear interaction between first-order eigenmodes at the still water level is significant and must not be neglected.

The amplitude of the second-harmonic free wave is large in shallow water and becomes less than 10% of the amplitude of the primary wave in deep water. Wavemakers with shallow draft (large d) generate free waves of larger amplitude in shallow and intermediate waver depths than the wavemakers with deep draft (small d). However, the opposite is predicted by theory in deep water. The ratio of the amplitude of the second-harmonic free wave to the amplitude of the second-harmonic Stokes wave (a_2^f/a_2^s) has minima between $.027<h/L_o<.06$ for flap-type wavemakers hinged on or above channel bottom and between $.06<h/L_o<.30$ for wavemakers hinged below the channel bottom. For flap-type wavemakers hinged on or above channel bottom, the ratio of a_2^f/a_2^s has maxima at $h/L_o=.16$.

Theoretical predictions on both the spatial dependence of the form and the meander phenome-

non of the resultant wave envelope along the horizontal distance due to existence of the second-harmonic free wave show good agreement with measured data obtained in a large-scale wave flume experiment.

ACKNOWLEDGMENT

The author wishes to express his thanks to Dr. Robert T. Hudspeth and Dr. A. Neil Williams for their valuable suggestions and discussions during this research. Numerical check by Dr. W. Sulisz of the Polish Academy of Sciences is gratefully acknowledged. Thanks are also due to the staffs of the OSU O.H. Hinsdale Wave Research Laboratory for their data acquisition and proffer for comparison with theoretical predictions. Financial support for this research was provided by the Korean Army, and it is gratefully acknowledged.

REFERENCES

1. Havelock, T.H., "Forced Surface Wave on Water", *Philosophical Magazine*, Vol. F, No.8, 1929, pp. 569 - 576.
2. Biesel, F., and Sequet, F., "Laboratory Wave Generating Apparatus". *Project Report* No.39. St. Anthony Falls Hydraulic Laboratory, University of Minnesota, Minneapolis, Minnesota, 1953.
3. Hyun, J.M. "Theory for Hinged Wavemakers of Finite Draft in Water of Constant Depth", *Journal of Hydronautics*, Vol.10, No.1, 1976, pp. 2 - 7.
4. Hudspeth, R.T., and Chen, M-C., "Design Curves for Hinged Wavemakers: Theory", *Journal of Hydraulics Division*, ASCE, Vol.107(HYS), 1981, pp. 533 - 552.
5. Goda, Y., and Kikuya, T., "The Generation of Water Waves with a Vertically Oscillating Flow at Channel Bottom", *Report No.9*, Port and Harbor Technical Research Institute, Ministry of Transportation, Japan(in English), 1964.
6. Multer, R.H., and Galvin, C.J., "Secondary Waves: Periodic Waves of Nonpermanent Form", (abstract) EOS *Transaction of the American Geophysical Union*, Vol. 48, 1967.
7. Iwagaki, Y., and Sakai, T., "Horizontal Water Particle Velocity of Finite Amplitude Waves", *Proceedings of the 12th Conference on Coastal Engineering*, ASCE, Washington, D.C., U.S.A., September 13-18,1970, pp.309 - 325.
8. Fontanet, P., "Th ories de la G n ration de la Houle Cylindrique par un Batteur Plan,", *La Houille Blanche*, Vol.16, No.1, 1961, pp. 3 - 31.
9. Madsen, O.S., "On the Generation of Long Waves," *Journal of Geophysical Research*, Vol.76, No. 36, 1971, pp. 8672 - 8683.
10. Multer, R.H., "Exact Nonlinear Model of Wave Generator", *Journal of the Hydraulics Division*, ASCE, Vol.99(HYI), 1973, pp.31 - 46.
11. Daugaard, "Generation of Regular Waves in the Laboratory", Doctoral Dissertation. Institute of Hydrodynamics Engineering, Technical University of Denmark, Copenhagen, Denmark, 1972.
12. Massel, S.R., "On the Nonlinear Theory of Mechanically Generated Waves in Laboratory Channels", *Mitteilungen Heft 70/1981*, Leichtweiss-Institut F r Wasserbau der Technischen Universitat Braunschweig, Germany (in German), 1981.
13. Flick, R.E., Guza, R.T., "Paddle Generated Waves in Laboratory Channels", *Journal of the Waterway, Port, Coastal and Ocean Division*, ASCE, Vol.106 (WW1), 1980, pp.79-97.
14. Kim, T-I and Hudspeth, R.T., "Nonlinear Fluid Forces on Hinged Wavemakers", *Journal of the Korean Society of Coastal and Ocean Engineers*, Vol.2, No.4, 1990, pp.208-222.
15. Goda, y. and Abe, Y., "Apparent Coefficients of Partial Reflection of Finite Amplitude Waves", *Report No.7(3)*, Port and Harbor Research Institute, Ministry of Transport, Japan, 1968.
16. Wehausen, J.V., "Surface Waves", in *Handbuch der Physik*. Volume 9, S. Flugge editor, Springer-Verlag, Berlin, 1960, pp. 446-757.
17. Stokes, G.G., "On the Theory of Oscillatory Waves", *Transactions of the Cambridge Philosophical Society*, London, England, Vol.8, 1847, pp.441-455.
18. Kim, T-I., Hudspeth, R.T., and Sulisz, W., "Circulation Kinematics in Nonlinear Laboratory Waves", *Proceedings of the 20th Conference on Coastal Engineering*, ASCE, Taipei, Taiwan, November 9-14, 1986, pp.381-395.
19. Buhr Hansen, J.B., and Svendsen, I.A., "Laboratory Generation of Waves of Constant Form", *Proceedings of the 14th Conference on Coastal Engineering*, ASCE, Copenhagen, Denmark, June 24-28, 1974, pp.321-339.
20. Dean, R.G., "Evaluation and Development of Wa-

ter Wave Theories for Engineering Application", Volume 1. *Special Report No.1*, U.S. Army Corps of Engineers, Coastal Engineering Research Center, Fort Belvoir, Virginia, U.S.A., 1974.

(接受 : 1992. 10. 28)

Appendix I. Coefficients for Second-Order Free Wave Potential, $_2\Phi^f$.

$$B_1=-\frac{ak\omega_o n_1^4}{2D^2(h)\beta_1^3}\sum_{m=2}^{\infty}\Big[\frac{D_m(\alpha_m)}{\alpha_m n_m(1+R_{m1}^2)^2}\{\phi_m(0)Q_1(0)\,[3\omega_o^2(h-d)(1+R_{m1}^2)$$
$$-4\frac{\omega_o^4}{\alpha_m^2}(1-R_{m1}^2)-2\rangle+I_1(d)\}+\frac{\beta_1 D(h)D_m(\alpha_m)}{n_1 n_m\alpha_m^2\sinh\ h[4+A_m^2(\alpha_m)]}\{2[F_{1m}+F_{2m}$$
$$-\alpha_m(F_{3m}+F_{4m})]\cdot[B_m(\alpha_m)-A_m(\alpha_m)]-[\alpha_m(F_{1m}+F_{2m})+F_{3m}+F_{4m}]$$
$$\cdot[4+A_m(\alpha_m)\cdot B_m(\alpha_m)]\}-\omega_o^2Q_1(0)\sum_{m=2}^{\infty}\frac{(1+\alpha/\alpha_m)D_m(\alpha_m)D(\alpha)}{n_m n\ \alpha_m\alpha^2[1+(R_{m1}+R_1)^2}$$
$$\cdot[2(1+\frac{\omega_o^4}{\alpha_m\alpha})+\frac{\alpha}{\alpha_m\ \cos^2\alpha\ h}]\phi_m(0)\,\phi_f(0)] \tag{51a}$$

$$B_n=-\frac{ak\omega_o n_1^4}{2D^2(h)\beta_n^3}\sum_{m=2}^{\infty}\Big[\frac{D_m(\alpha_m)}{\alpha_m n_m(1+R_{mn}^2)^2}\{\phi_m(0)Q_n(0)\,[3\omega_o^2(h-d)(1+R_{mn}^2)$$
$$-4\frac{\omega_o^4}{\alpha_m^2}(1-R_{mn}^2)-2\rangle+I_2(d)\}+\frac{\beta_n D(h)D_m(\alpha_m)}{n_1 n_m\alpha_m^2\sinh\ h[4+A_m^2(\alpha_m)]}\{2[F_{5m}+F_{6m}$$
$$-\alpha_m(F_{7m}+F_{8m})]\cdot[B_m(\alpha_m)-A_m(\alpha_m)]-[\alpha_m(F_{5m}+F_{6m})+F_{7m}+F_{8m}]$$
$$\cdot[4+A_m(\alpha_m)\cdot B_m(\alpha_m)]\}-\omega_o^2Q_n(0)\sum_{m=2}^{\infty}\frac{(1+\alpha/\alpha_m)D_m(\alpha_m)D(\alpha)}{n_m n\ \alpha_m\alpha^2[1+(R_{mn}+R_n)^2}$$
$$\cdot[2(1+\frac{\omega_o^4}{\alpha_m\alpha})+\frac{\alpha}{\alpha_m\ \cos^2\alpha\ h}]\phi_m(0)\,\phi(0)] \tag{51b}$$

$$C_1=\frac{4ak\omega_o}{\beta_1^3}\Big[\frac{3Q_1(0)}{2(1-4\beta_1^{-2})\sinh\ 2h}-\frac{n_1^3}{8D(h)(1-\beta_1^{-2})^2\ \sinh\ h}\cdot\{\phi_1(0)Q_1(0)[3\omega_o^2(h-d)(1-\beta_1^{-2})$$
$$+4\omega_o^4(1+\beta_1^{-2})-2]+I_3(d)\}+\sum_{m=2}^{\infty}\frac{n_1^3D_m(\alpha_m)}{8D(h)\sinh\ h\ n_mR_{m1}[4+A_m^2(\alpha_m)]}$$
$$\cdot[B_m(\alpha_m)-A_m(\alpha_m)+[\alpha^{-1}(F_{1m}+F_{2m})-F_{3m}-F_{4m}]\cdot[4+A_m(\alpha_m)\cdot B_m(\alpha_m)]\}] \tag{51c}$$

$$C_n=\frac{4ak\omega_o}{\beta_n^3}\Big[\frac{3Q_n(0)}{2(1-4\beta_n^{-2})\sinh\ 2h}-\frac{n_1^3}{8D(h)(1-\beta_n^{-2})^2\ \sinh\ h}\cdot\{\phi_1(0)Q_n(0)[3\omega_o^2(h-d)(1-\beta_n^{-2})$$
$$+4\omega_o^4(1+\beta_n^{-2})-2]+I_4(d)\}+\sum_{m=2}^{\infty}\frac{n_1^3D_m(\alpha_m)}{8D(h)\sinh\ h\ n_mR_{mn}[4+A_m^2(\alpha_m)]}$$
$$\cdot[B_m(\alpha_m)-A_m(\alpha_m)+[\alpha^{-1}(F_{5m}+F_{6m})-F_{7m}-F_{8m}]\cdot[4+A_m(\alpha_m)\cdot B_m(\alpha_m)]\}] \tag{51d}$$

in which $R_{m1}=\alpha_m/\beta_1$, $R_{mn}=\alpha_m/\beta_n$, $R_{\ n}=\alpha/\beta_n$; and

$$I_1(d)=\begin{cases}-\ \phi_m(d-h)Q_1(d-h)[2-R_{m1}^{-1}(1-R_{m1}^2)\tan\ \alpha_m d\cdot\tanh\beta_1 d] & \text{for } d\geq 0\\ -\ 2/(n_mN_1) & \text{for } d<0\end{cases} \tag{51e}$$

$$I_2(d)=\begin{cases}-\phi_m(d-h)Q_n(d-h)[2+R_{mn}^{-1}(1-R_{mn}^2)\tan\alpha_m d\cdot\tanh\beta_n d] & \text{for } d\geq 0\\ -2/(n_m N_n) & \text{for } d<0\end{cases} \tag{51f}$$

$$I_3(d)=\begin{cases}-\phi_1(d-h)Q_n(d-h)[2-\beta_1(1-\beta_1^{-2})\tanh d\cdot\tanh\beta_1 d] & \text{for } d\geq 0\\ -2/(n_1 N_1) & \text{for } d<0\end{cases} \tag{51g}$$

$$I_4(d)=\begin{cases}-\phi_1(d-h)Q_n(d-h)[2+\beta_n(1-\beta_n^{-2})\tanh d\cdot\tanh\beta_n d] & \text{for } d\geq 0\\ -2/(n_1 N_n) & \text{for } d<0\end{cases} \tag{51h}$$

and

$$F_{1m}=\phi_1'(0)\phi_m(0)Q_1(0)[(1+\beta_1^{-1})(1+4\beta_1^{-1})-\beta_1^{-1}(1+4\omega_o^4\beta_1^{-1})]/[(1+\beta_1^{-1})^2+R_{m1}^2] \tag{51i}$$

$$F_{2m}=-\phi_1'(0)\phi_m(0)Q_1(0)[(1-\beta_1^{-1})(1-4\beta_1^{-1})+\beta_1^{-1}(1-4\omega_o^4\beta_1^{-1})]/[(1-\beta_1^{-1})^2+R_{m1}^2] \tag{51j}$$

$$F_{3m}=-\phi_1'(0)\phi_m(0)Q_1(0)[\alpha_m^{-1}(1+\beta_1^{-1})(1+4\omega_o^4\beta_1^{-1})+R_{m1}((1+4\beta_1^{-1})]/[(1+\beta_1^{-1})^2+R_{m1}^2] \tag{51k}$$

$$F_{4m}=\phi_1'(0)\phi_m(0)Q_1(0)[\alpha_m^{-1}(1-\beta_1^{-1})(1+4\omega_o^4\beta_1^{-1})-R_{m1})(1-4\beta_1^{-1})]/[(1-\beta_1^{-1})^2+R_{m1}^2] \tag{51l}$$

$$F_{5m}=\phi_1'(0)\phi_m(0)Q_n(0)[\beta_n^{-1}(1-4\omega_o^4\alpha_m^{-1}\beta_n^{-1})-(1+R_{mn})(\alpha_m^{-1}+4\beta_n^{-1})]/[(1+R_{mn})^2+\beta_n^{-2}] \tag{51m}$$

$$F_{6m}=\phi_1'(0)\phi_m(0)Q_n(0)[\beta_n^{-1}(1+4\omega_o^4\alpha_m^{-1}\beta_n^{-1})+(1-R_{mn})(\alpha_m^{-1}-4\beta_n^{-1})]/[(1-R_{mn})^2+\beta_n^{-2}] \tag{51n}$$

$$F_{7m}=-\phi_1'(0)\phi_m(0)Q_n(0)[\beta_n^{-1}(\alpha_m^{-1}+4\beta_n^{-1})+(1+R_{mn})(-4\omega_o^4\alpha_m^{-1}\beta_n^{-1})]/[(1+R_{mn})^2+\beta_n^{-2}] \tag{51o}$$

$$F_{8m}=\phi_1'(0)\phi_m(0)Q_n(0)[-\beta_n^{-1}(\alpha_m^{-1}-4\beta_n^{-1})+(1-R_{mn})(+4\omega_o^4\alpha_m^{-1}\beta_n^{-1})]/[(1-R_{mn})^2+\beta_n^{-2}] \tag{51p}$$

Appendix II. Notations

a, a_2^s, a_2^f	First-order, second-order Stokes, and free wave amplitudes, respectively
d	Height of wavemaker hinge above the bottom
e	Height of wavemaker piston measured above the wavemaker hinge
g	Gravitational acceleration
H	Wave height
i, j	Unit horizontal and vertical vectors, respectively
h	Still water depth of the channel
$k(=\frac{2\pi}{L})$, k_m	Wave number for the linear propagating and evanescent eigenmodes, respectively
L, $L_o(=\frac{g}{2\pi}T_2)$	Wavelengths in finite depth and in deep water, respectively
L_b	Beat (meander) wavelength in the second-harmonic wave
n_m, N_m	Normalizing constants for the linear and second-order eigenfunctions, respectively
p	pressure
Q_1, Q_m	Orthonormal eigenfunctions for the second-order solution
q_1, q_m	Propagating and evanescent wave number for the second-order free wave potential
S/2	Wavemaker stroke
T	Wave period
U(·)	Heaviside step function
u, v	Eulerian horizontal and vertical velocity components, respectively
x, y	Horizontal and vertical Cartesian coordinate axes, respectively, with origin located at undisturbed water level at wavemaker

Greek

α_m	Dimensionless eigenvalues at first-order
β_1, β_m	Dimensionless eigenvalues at second-order